ARTICLE

Experimental and computational investigations on ring-opening polymerization mechanisms of amide-functional benzoxazines

Wenqian Zhao[1] · Richie Yang[2] · Shengfu Yang[3] · Kan Zhang[1]

Abstract

We observed an unusual low polymerization temperature for the *ortho*-amide benzoxazine in comparison with its *para*-isomer. Density functional theory (DFT) calculations suggested that the intramolecular hydrogen bond between the oxazine ring and the adjacent amide softens the C–O bond, resulting in a reduced activation energy and thus a low ring-opening polymerization temperature. In addition, the polymerization kinetics of both *para*- and *ortho*-amide functional benzoxazines were investigated using the Starink method, which confirmed a relatively lower activation energy for the *ortho*-amide functional benzoxazine compared with its *para*-isomer. Our work suggests that softening chemical bonds by intramolecular hydrogen bonding may become a new strategy for the design of high-performance polybenzoxazine thermosets with low processing temperatures.

Graphical abstract

Graphical abstract

The combination of experimental and computational investigations provides deeper molecular-level insights of the polymerization mechanisms in smart *ortho*-amide benzoxazines.
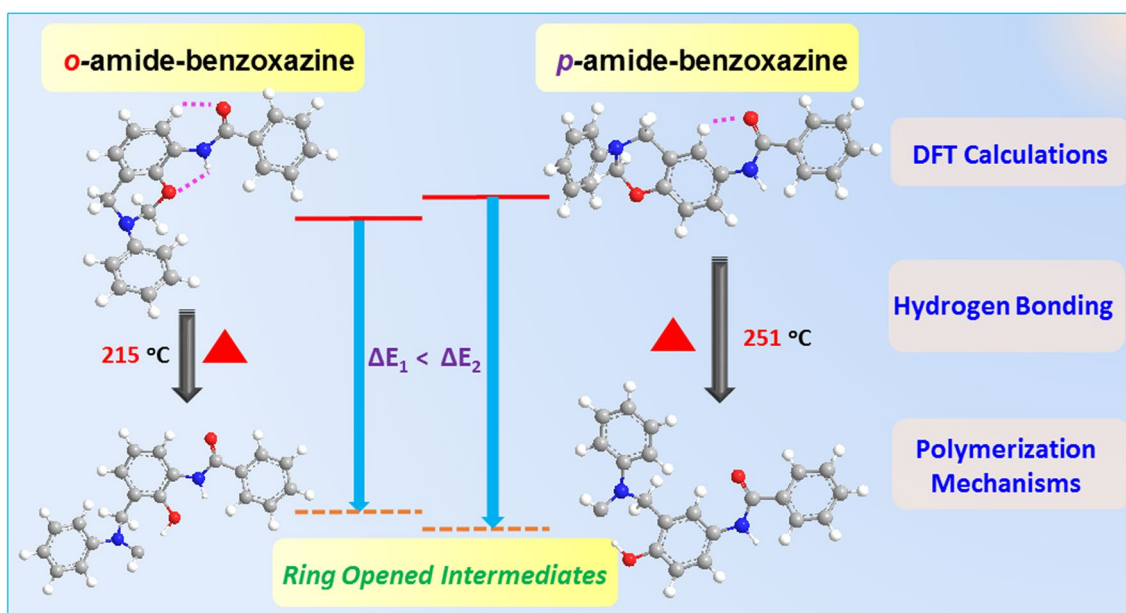
Keywords Benzoxazine · Amide · Hydrogen bonding · Polybenzoxazine · Polymerization kinetics

Extended author information available on the last page of the article

1 Introduction

Benzoxazine is a thermosetting resin that can be readily synthesized via Mannich condensation from the starting materials of phenol, formaldehyde/paraformaldehyde and amine [1, 2]. It has been extensively explored due to the excellent properties that it possesses, such as easy synthesis and low cost [3–5]. Its polymeric product, namely polybenzoxazine, merits low surface free energy [6–8], low dielectric constant [9, 10], and excellent thermal and mechanical properties [11–14]. The most attractive characteristic of polybenzoxazines is, however, the very high degree of flexibility in molecular design, which allows to tailor the structures to achieve desired performance [2].

The typical terminal polymerization temperature for processing benzoxazine resins in absence of catalysts/initiators is over 220 °C [15] but many applications require a lower polymerization temperature. Hence, a number of functional groups have been added into benzoxazines to lower the polymerization temperature, such as acidic compounds [16–18], basic compounds [19–21], combinations of acids and bases [22, 23], and metal-containing compounds[24]. However, most reported promoting effects are attributed to additives; while the catalytic effect on the ring-opening polymerization based on the functionality from benzoxazine itself has rarely been investigated. Andreu et al. evaluated the electronic effects on the polymerization temperature by several mono-benzoxazine compounds with electron-donating or electron-withdrawing groups [25]. Lately, Wang et al. reported the electronic and bridging effects on the ring-opening polymerization of bis-benzoxazine resins [26]. They noted that the electron-withdrawing groups could accelerate the polymerization process, leading to a relatively lower activation energy and curing temperature by reducing the bond energy of C–O bond from oxazine rings.

Recently, *ortho*-amide benzoxazine resins are found to polymerize at much lower temperatures than many well-known pure benzoxazines without the addition of any initiators or catalysts [27, 28]. Froimowicz et al. provided solid evidences for the presence of intramolecular five-membered-ring hydrogen bonding in *ortho*-amide benzoxazines using NMR and FT-IR experiments [29, 30]. The intramolecular hydrogen bonding between the oxazine ring and the adjacent amide linkage was supposed to be an internal incentive to promote the ring-opening polymerization in a smart way, mimicking a self-catalytic effect. Nevertheless, the roles of intramolecular hydrogen bonding in ring-opening polymerization for amide-containing benzoxazine resins remains unclear.

In the current study, we synthesized both *para*- and *ortho*-amide functional benzoxazine isomers, *p*HBA-a and *o*HBA-a (Fig. 1), and investigated the intramolecular hydrogen bonding using DFT calculations, in order to obtain molecular-level insights on how intramolecular hydrogen bonding influences the ring-opening polymerization of *ortho*-amide functional benzoxazines. To validate the computational investigation, the activation energies of polymerization for both *p*HBA-a and *o*HBA-a have also been retrieved according to the DSC experiments.

2 Experimental

2.1 Materials

p-Aminophenol (98%), *o*-Aminophenol (98%), paraformaldehyde (96%), benzoyl chloride and phenol (98%) were used as received from Aladdin Reagent, China. Sodium sulfate, aniline, hexane, chloroform, sodium hydroxide (NaOH), 1,4-dioxane, lithium chloride (LiCl) and ethyl acetate, were obtained from Macklin, China. and used as

Fig. 1 Optimized structures of *p*HBA-a (**a**) and *o*HBA-a (**b**)
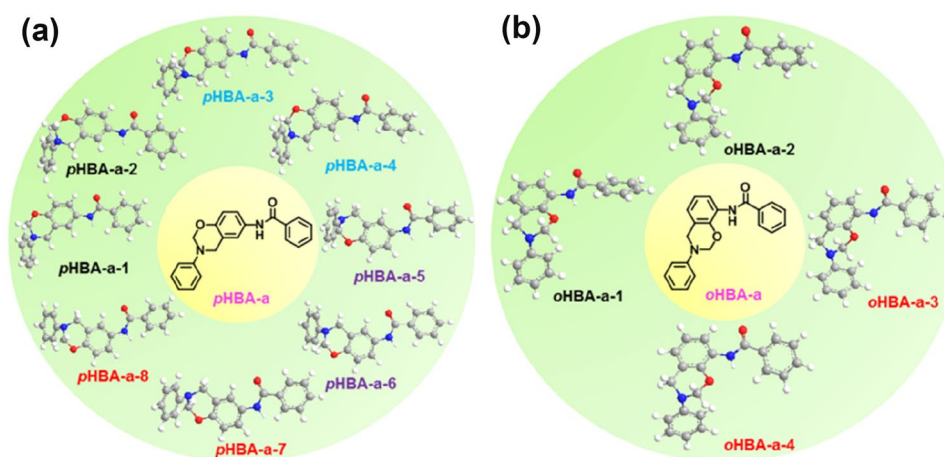
Scheme 1 Synthesis of Benzo-xazine Monomers
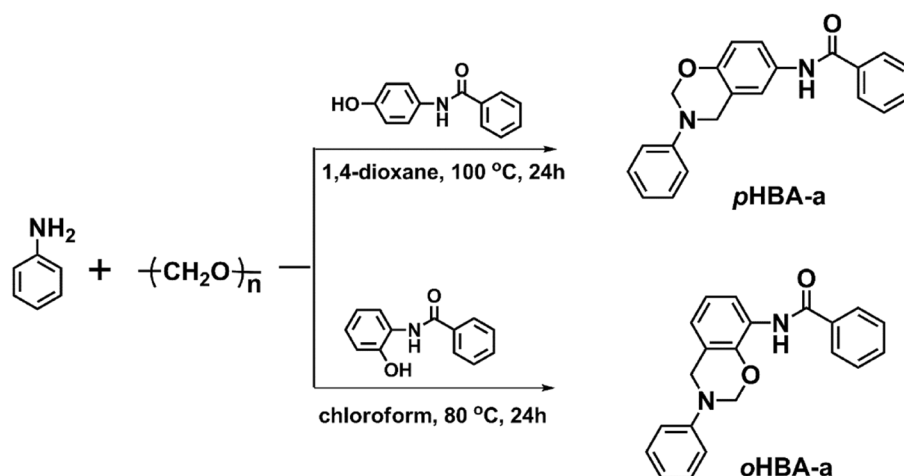
received. *N*-(4-hydroxyphenyl) benzamide and *N*-(2-hydroxyphenyl) benzamide were synthesized according to the previously reported method [31].

2.2 Synthesis of N-(3-phenyl-3,4-dihydro-2*H*-benzo[e][1,3] oxazin-6-yl)benzamide (Abbreviated as *p*HBA-a)

1,4-Dioxane was used as the solvent. Aniline (1.32 g, 14.10 mmol), *N*-(4-hydroxyphenyl) benzamide (3.00 g, 14.10 mmol), and paraformaldehyde (0.69 g, 28.20 mmol) were added into a 250 mL round-bottom flask equipped with a condenser. The mixture was stirred at 100 °C for 24 h, then the mixture was cooled to room temperature. The reaction mixture was poured into 250 mL of cold water to give a powder like precipitate. The product was dissolved in ethyl acetate and further purified by washing with 0.5 N NaOH solution and distilled water to eliminate the residual starting materials. Finally, the crude products were dried over sodium sulfate followed by fractionating with the column chromatography (eluent: hexanes and ethyl acetate, volume ratio = 3:1) to obtain pure final product (yield 73%). ^{1}H NMR (DMSO-d$_6$), ppm: $\delta = 4.64$ (s, Ar–CH$_2$–N, oxazine), 5.42 (s, O–CH$_2$–N, oxazine), 6.70–7.91 (13H, Ar), 10.07 (s, NH). IR spectra (KBr), cm^{-1}: 1646 (amideI), 1227 (C–O–C asymmetric stretching), 940 (out-of-plane C–H of benzene ring to which oxazine ring is attached).

2.3 Synthesis of N-(3-phenyl-3,4-dihydro-2*H*-benzo[e][1,3] oxazin-8-yl)benzamide (Abbreviated as *o*HBA-a)

50 mL of chloroform, aniline (1.32 g, 14.10 mmol), paraformaldehyde (0.69 g, 28.20 mmol) and *N*-(2-hydroxyphenyl) benzamide (3.00 g, 14.10 mmol) were mixed in a round flask. The mixture was stirred with a magnetic stirrer

at 80 °C for 24 h, and then cooled to room temperature. Subsequently, the solution was purified by washing with cold water. The chloroform solution was dried over sodium sulfate anhydrous to obtain crude product. Crude product was fractionated by the column chromatography (eluent: hexanes and ethyl acetate, volume ratio = 3:1) to obtain
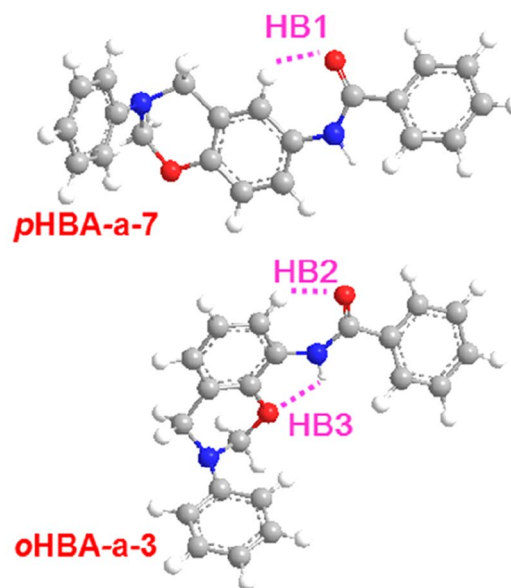
Bond Name	E_HB (kcal/mol)
HB1	3.07
HB2	3.03
HB3	3.59

Fig. 2 Hydrogen bonding systems and calculated hydrogen bond energy values in *p*HBA-a-7 and *o*HBA-a-3

Fig. 3 Calculations for the oxa-zine-ring ring-opened reaction of *o*HBA-a-3 and *p*HBA-a-7
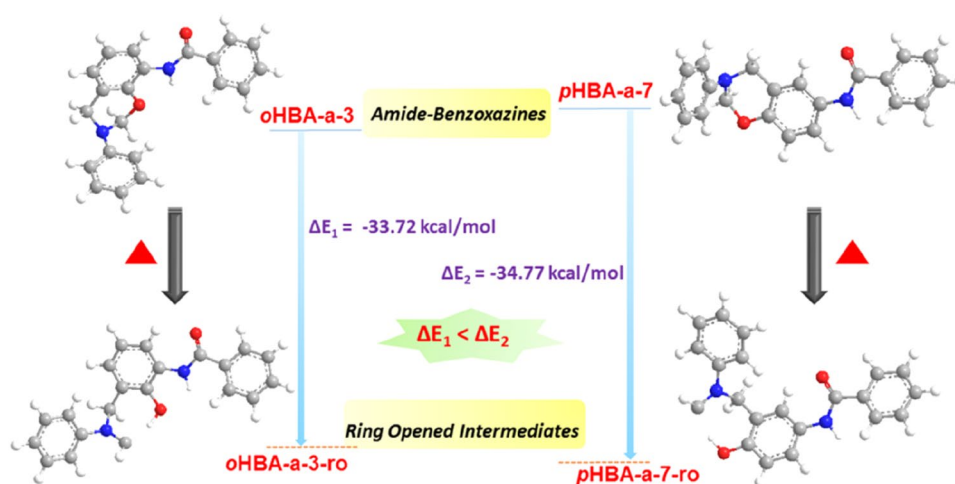
2.4 Characterization

^{1}H and ^{13}C nuclear magnetic resonance (NMR) spectra were acquired on Bruker AVANCE II NMR 400 MHz spectrometer. The average numbers of transients for ^{1}H and ^{13}C NMR measurements were 64 and 1024, respectively. Fourier transform infrared (FT-IR) spectra were recorded with a Nicolet Nexus 670 FT-IR Spectrometer. Coaddition of 64 scans was recorded at a resolution of 4 cm^{-1}. Differential scanning calorimetry (DSC) is used to study the polymerization behavior of the prepared samples using NETZSCH Model 204f1 DSC and was used with a heating rate of 10 °C/min and a nitrogen flow rate of 60 mL/min. In the analyses to determine the activation energy of benzoxazine polymerization, the samples (2.0 ± 0.5 mg) were scanned at different heating rates of 2, 5, 10, 15, 20 °C/min.

2.5 Computational methods

Quantum chemical calculations were performed using both the Gaussian16 quantum chemical computational package [32]. The B3LYP hybrid functional was employed using a 6–311 + + G(d, p) basis set, with the GD3 empirical dispersion to account for the weak intramolecular interactions. Chemical structures of benzoxazine monomers were optimized and the harmonic vibrational frequencies were determined to show that true structural minima had been found. The intramolecular hydrogen bonding energies were calculated based on all-electron densities at critical bond points using the method reported elsewhere [33]

3 Results and discussion

Amide-functional benzoxazine monomers, *p*HBA-a and *o*HBA-a, were synthesized by Mannich condensation from N-(4-hydroxyphenyl) benzamide/N-(2-hydroxyphenyl) benzamide, aniline and paraformaldehyde (Scheme 1). Both benzoxazine monomers were carefully purified, and their chemical structures were confirmed by NMR and FT-IR spectra (see Figures S1–S3, Supporting Information). DFT calculations found eight configurations with near identical total energies for *p*HBA-a, as shown in Fig. 1a. These configurations are determined by three folds, i.e., (1) the oxygen from the carbonyl is located on either side of the oxygen in oxazine ring; (2) the tilt of the terminal benzene ring attached to C=O relative to the plane of amide group; (3) the benzene ring attached to the nitrogen in oxazine ring is bent above or below the oxazine ring. Besides, the eight configurations can be divided into four sets, and the configurations in each set has exactly the same total energy. Configurations *p*HBA-a-7 and *p*HBA-a-8 show the lowest energy possessing most stable structures. *o*HBA-a, in contrast, has only four configurations (see Fig. 1b) as the *cis* location of the two oxygen atoms is unfavoured due to electrostatic repulsion; so the fold (1) from *p*HBA-a is not compliant. Similar to *p*HBA-a, two configurations possess the same energy, with *o*HBA-a-3 and *o*HBA-a-4 being the lowest energy structure. A summary of the total energy for each structure is provided in Table S1.

As seen from the optimized molecular structures, intramolecular six-membered ring hydrogen bonds (HB1 and HB2 in Fig. 2) are likely formed between the aromatic proton from benzoxazine and the oxygen from amide in both *p*HBA-a-7 and *o*HBA-a-3; and an extra intramolecular five-membered ring hydrogen bond (HB3 in Fig. 2) is possible between the oxazine ring and the adjacent amide linkage in *o*HBA-a. To confirm this, the hydrogen bond energy (EHB) in each benzoxazine was calculated based on all-electron
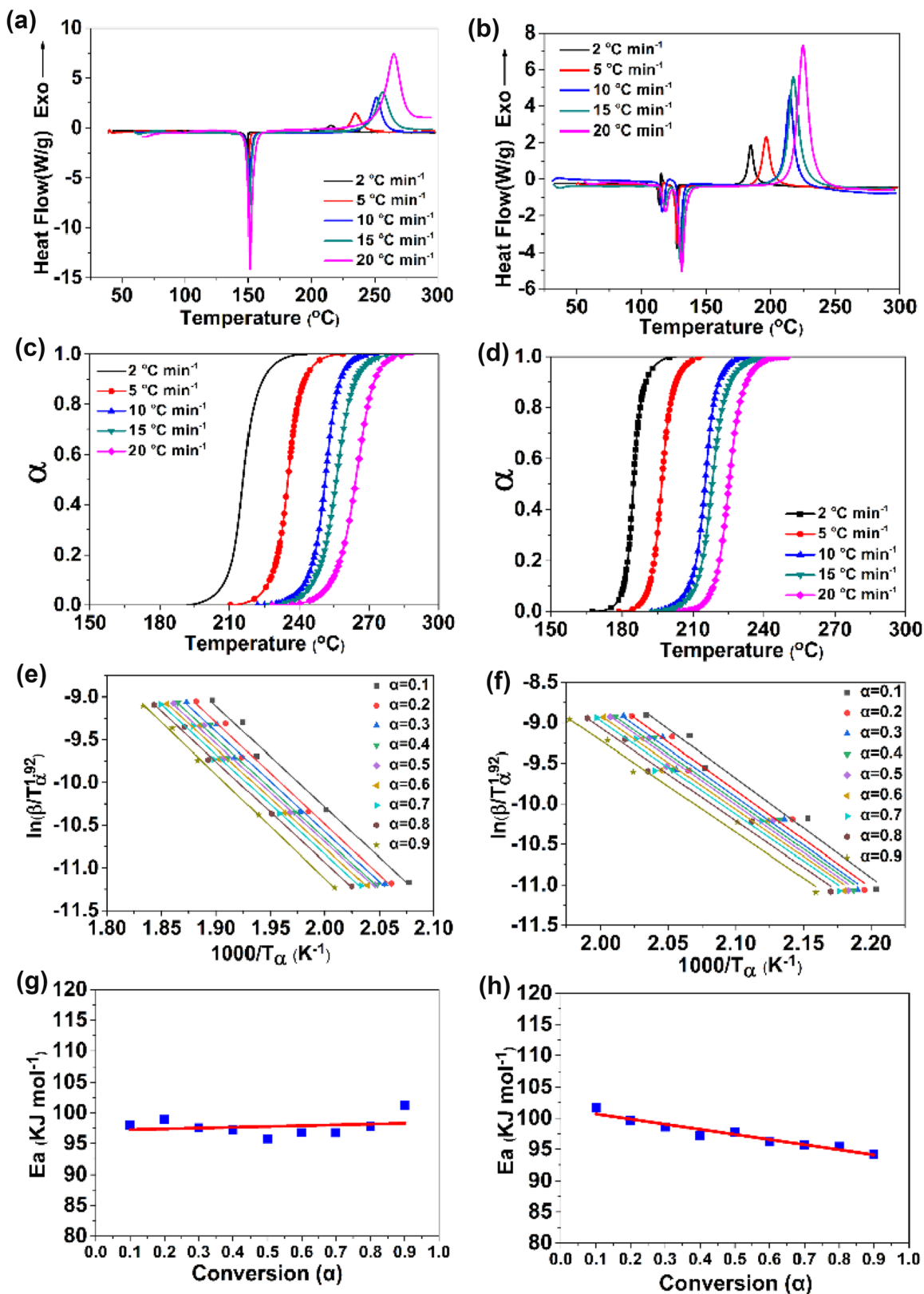
pure final product (yield 80%). ^{1}H NMR (DMSO-d$_6$), ppm: δ = 4.68 (s, Ar–CH$_2$–N, oxazine), 5.45 (s, O–CH$_2$–N, oxazine), 6.87–7.94 (13H, Ar), 9.35 (s, NH). IR spectra (KBr), cm^{-1}: 1666 (amideI), 1237 (C–O–C asymmetric stretching), 921 (out-of-plane C–H of benzene ring to which oxazine ring is attached).

Fig. 4 DSC thermograms of *p*HBA-a (**a**) and *o*HBA-a (**b**) at different heating rates. Conversion *versus* temperature for *p*HBA-a (**c**) and *o*HBA-a (**d**) cured at different heating rates. Variation of *versus* 1000/ T_{α} for *p*HBA-a (**e**) and *o*HBA-a (**f**). E_a as a function of the polymerization conversion of *p*HBA-a (**g**) and *o*HBA-a (**h**)

density at bond critical points using the Multiwfn software [33]. As shown in Fig. 2, a stronger hydrogen bond is present in *o*HBA-a when compared the six-membered ring hydrogen bonds in both *o*HBA-a and *p*HBA-a, which is consistent with the previously reported experimental results [29].

The *ortho*-amide functional mono-benzoxazine, *o*HBA-a, is shown to polymerize at much lower temperature than *p*HBA-a (Figure. S4). This suggests that the intramolecular hydrogen bonding, HB3, may act as an incentive to activate the ring-opening polymerization for *o*HBA-a. In other words, the existence of the HB3 weakens the bond of O–CH$_2$, leading to a relatively lower energy for breaking this oxazine ring bond. To confirm this speculation, we analyzed the real-space functions at the bond critical points of the C–O bond using the Multiwfn software, which showed the all-electron densities for the C–O bond in *p*HBA-a and *o*HBA-a as 0.241 e Å^{-3} and 0.235 e Å^{-3}, respectively, suggesting a stronger C–O bond in *p*HBA-a than *o*HBA-a. In addition, we also checked the local potential energy densities (LPE) of the O–CH$_2$ bonds in the benzoxazine rings. LPE is calculated based on the Coulomb's law for two charged particles, which is a measure for the strength of intra/intermolecular interactions of dimers or complexes by means of the charge density at the bond critical point and effective charge of the atoms involved in these interactions, and is known to correlate linearly with the intra/intermolecular binding energy [34]. LPEs were found to be –297.4 and –288.0 kcal/mol for *p*HBA-a and *o*HBA-a, respectively, where a more negative potential energy density for *p*HBA-a means a stronger bonding between its C–O bond compared with that in oHBA-a. Indeed, this is also reflected by bond length: the C–O bond in *o*HBA-a (1.45526 Å) is slightly longer than that in *p*HBA-a (1.44805 Å), which is also consistent with the softened C–O bond in *o*HBA-a. Although the changes in these quantities are marginal (by 2–3%), they have exhibited significant influence on the polymerization temperature. We also paid attention to the torsional interactions in ring structures of oxazine ring. DFT calculations showed that the torsional motion of –CH$_2$ (next to the O atom) of the oxazine ring in *o*HBA-a exhibits a slightly higher frequency than *p*HBA-a, making it easier to reach the transition state of the ring-opening reactions (see below).

To further establish the effect of intramolecular hydrogen bonding in *o*HBA-a, we performed calculations on the oxazine ring-open reaction. As shown in Fig. 3, the energy barrier between *o*HBA-a-3 and its corresponding ring-opened intermediate, *o*HBA-a-3-ro, was found to be 33.72 kcal/mol; while this activation energy between *p*HBA-a-7 and its ring-opened intermediate (*p*HBA-a-7-ro) is 34.77 kcal/mol. It is therefore conclusive that *o*HBA-a has a weaker O-CH$_2$ bond than that in *p*HBA, which can only be attributed to the intramolecular hydrogen bonding between the oxazine ring and the amide linkage.

At last, we derived the activation energy values for the ring-opening polymerization of both *p*HBA-a and *o*HBA-a using DSC measurements. Figure 4a, b, and c, d show the DSC curves of *p*HBA-a and *o*HBA-a and their conversion versus temperature at different heating rates, respectively. The kinetics for the non-isothermal polymerization of *p*HBA-a and *o*HBA-a are conducted using the rate equation as follows:

$$\frac{\mathrm{d}\alpha}{\mathrm{d}t} = k(T)f(\alpha), \tag{1}$$

where α is the rate for the ring-opening polymerization process of conversion, $f(\alpha)$ is the differential conversion function corresponding to the polymerization mechanisms, and $k(T)$ is a rate constant depended on temperature, which can be obtained using the Arrhenius equation:

$$k(T) = A\exp\left(\frac{-E_a}{\mathrm{R}T}\right), \tag{2}$$

where E_a is the activation energy and A is a constant.

The E$_a$ values of *p*HBA-a and *o*HBA-a were calculated by Starink method because this theory can reflect how E_a varies with conversion [35, 36]. Besides, the Starink method shows as multi-step kinetics which results in a set of E_a values rather than only a single-step kinetic as observed from Kissinger or Ozawa methods [37, 38]. The Starink method equation is as follows,

$$\ln\left(\beta/T_\alpha^{1.92}\right) = C - 1.0008\frac{E_a}{\mathrm{R}T_\alpha}, \tag{3}$$

where β is the heating rate and T_α represents the temperature at conversion α. The combination of the above results led to obtain Fig. 4e and Fig. 4f by plotting as a function of 1000/T_α. Therefore, the E_a valufunction of 1000es of *p*HBA-a and *o*HBA-a as a function of the conversion can be obtained as shown in Fig. 4g and Fig. 4h, respectively. The average activation energy values for *p*HBA-a and *o*HBA-a were calculated as 23.60 and 23.25 kcal/mol, respectively. Therefore, the experimental result indicates the relatively higher activation energy value of *p*HBA-a.

4 Conclusions

In summary, two amide-functional benzoxazines were successfully synthesized. The presence of intramolecular hydrogen bonding in both amide-containing benzoxazines were confirmed using DFT calculations, which agreed with the

previously reported experiments. We confirmed that a lower polymerization temperature for *o*HBA-a is attributed to the intramolecular hydrogen bonding between the amide hydrogen and the oxygen atom in the oxazine ring. The presence of such an intramolecular hydrogen bond reduces the total electron density between the O–CH$_2$ bond and, thus, lowers the bonding energy, making it easy for ring-open polymerization to occur in *o*HBA-a. The same strategy can be applied to soften the O–CH$_2$ bond in benzoxazines and can, thus, reduce the polymerization temperature. Moreover, the *ortho*-amide functional benzoxazine exhibited a relatively lower activation energy compared with its *para*-isomer based on the Starink method, which agrees with the DFT calculations. This work, therefore, adds a new angle to the molecular design principle for the benzoxazine families.

Declarations

Conflict of interest The authors declare no competing financial interest.

References

1. Y. Lu, Y. Zhang, K. Zhang, Chem. Eng. J. **448**, 137670 (2022)
2. X. Ning, H. Ishida, J. Polym. Sci. Part A Polym. Chem. **32**, 1121 (1994)
3. H. Ishida, *Handbook of Benzoxazine Resins* (Elsevier, Amsterdam, 2011)
4. N.N. Ghosh, B. Kiskan, Y. Yagci, Prog. Polym. Sci. **32**, 1344 (2007)
5. H. Ishida, P. Froimowicz, Elsevier: Amsterdam, (2017).
6. Y. Lyu, H. Ishida, Prog. Polym. Sci. **99**, 101168 (2019)
7. C.F. Wang, Y.C. Su, S.W. Kuo, C.F. Huang, Y.C. Sheen, F.C. Chang, Angew. Chem. Int. Ed. **45**, 2248 (2006)
8. S.W. Kuo, Y.C. Wu, C.F. Wang, K.U. Jeong, J. Phys. Chem. C. **113**, 20666 (2009)
9. C.S. Liao, C.F. Wang, H.C. Lin, H.Y. Chou, F.C. Chang, J. Phys. Chem. C. **112**, 16189 (2008)
10. K. Zhang, X. Yu, S.W. Kuo, Polym. Chem. **10**, 2387 (2019)
11. J. Wu, Y. Xi, G.T. Mccandless, Y. Xie, R. Menon, Y. Patel, R. Menon, Y. Patel, D.J. Yang, S.T. Iacono, B.M. Novak, Macromolecules **48**, 6087 (2015)
12. Y. Lu, K.W.J. Ng, H. Chen, X. Chen, S.K.J. Lim, W. Yan, X. Hu, Chem. Commun. **57**, 3375 (2021)
13. K. Zhang, X. Yu, Macromolecules **51**, 6524 (2018)
14. Y. Lu, X.Y. Yu, C.J. Evans, S.F. Yang, K. Zhang, Polym. Chem. **21**, 5059 (2021)
15. S. Mukherjee, B. Lochab, Chem. Commun. **58**, 3609 (2022)
16. L. Han, M.L. Salum, K. Zhang, P. Froimowicz, H. Ishida, J. Polym. Sci. Part A Polym. Chem. **55**, 3434 (2017)
17. S. Miura, N. Kano, Jpn. Kokai. Tokkyo. Koho., Patent, 2000178332A2 (2000).
18. S. Miura, N. Kano, Jpn. Kokai. Tokkyo. Koho., Patent, 2001213967A2 (2001).
19. S. Miura, Jpn. Kokai. Tokkyo. Koho., Patent, 2003082099A2 (2003).
20. T. Orihara, Jpn. Kokai. Tokkyo. Koho., Patent, 200086863A1 (2000).
21. J.Q. Sun, W. Wei, Y.Z. Xu, J.H. Qu, X.D. Liu, T. Endo, RSC. Adv. **5**, 19048 (2015)
22. K. Zhang, R. Cai, Q. Zhuang, X. Liu, G. Yang, Z. Han, J. Polym. Sci. Part A Polym.Chem. **52**, 1514 (2014)
23. A. Sudo, R. Kudoh, H. Nakayama, K. Arima, T. Endo, Macromolecules **41**, 9030 (2008)
24. H. Kimura, A. Matsumoto, K. Ohtsuka, J. Appl. Polym. Sci. **109**, 1248 (2008)
25. Y.X. Wang, H. Ishida, Polymer **40**, 4563 (1999)
26. R. Andreu, J.A. Reina, J.C. Ronda, J. Polym. Sci. Part A Polym Chem. **46**, 3353 (2008)
27. X.Y. Wang, P. Chen, Y. Gu, J. Polym. Sci. Part A Polym. Chem. **49**, 1443 (2011)
28. T. Agag, J. Liu, R. Graf, H.W. Spiess, H. Ishida, Macromolecules **45**, 8991 (2012)
29. K. Zhang, L. Han, P. Froimowicz, H. Ishida, Macromolecules **50**, 6552 (2017)
30. P. Froimowicz, K. Zhang, H. Ishida, Chem. Eur. J. **22**, 2691 (2016)
31. L. Han, K. Zhang, H. Ishida, P. Froimowicz, Macromol. Chem. Phys. **218**, 1600562 (2017)
32. M.J. Frisch, G.W. Trucks, H.B. Schlegel, G.E. Scuseria, M.A. Robb, J.R. Cheeseman, G. Scalmani, V. Barone, G.A. Petersson, H. Nakatsuji, X. Li, M. Caricato, A.V. Marenich, J. Bloino, B.G. Janesko, R. Gomperts, B. Mennucci, H.P. Hratchian, J. V. Ortiz, A.F. Izmaylov, J.L. Sonnenberg, D. Williams-Young, F. Ding, F. Lipparini, F. Egidi, J. Goings, B. Peng, A. Petrone, T. Henderson, D. Ranasinghe, V.G. Zakrzewski, J. Gao, N. Rega, G. Zheng, W. Liang, M. Ada, M. Ehara, K. Toyota, R. Fukuda, J. Hasegawa, M. Ishida, T. Nakajima, Y. Honda, O. Kitao, H. Nakai, T. Vreven, K. Throssell, J.A. Jr. Montgomery, J.E. Peralta, F. Ogliaro, M.J. Bearpark, J.J. Heyd, E.N. Brothers, K.N. Kudin, V.N. Staroverov, T.A. Keith, R. Kobayashi, J. Normand, K. Raghavachari, A.P.; Rendell, J.C. Burant, S.S. Iyengar, J. Tomasi, M. Cossi, J.M. Millam, M. Klene, C. Adamo, R. Cammi, J.W. Ochterski, R.L. Martin, K. Morokuma, O. Farkas, J.B. Foresman and D.J. Fox, Gaussian 16, Revision C.01, Gaussian, Inc., Wallingford CT., (2016).
33. S. Emamian, T. Lu, H. Kruse, H.J. Emamian, J. Comput. Chem. **40**, 2868 (2019)
34. G.L. Firme, Comp. Theo. Chem. **197**, 113143 (2021)
35. T. Zhang, J. Wang, M. Derradji, N. Ramdani, H. Wang, Z.W. Lin, W.B. Liu, Thermochim. Acta. **602**, 22 (2015)
36. L. Sun, K. Zhang, C.Y. Min, Y.Q. Liu, Y.T. Wang, J.X. Zhang, S.J. Li, Thermochim. Acta. **668**, 1 (2018)
37. H.E. Kissinger, Anal. Chem. **29**, 1702 (1957)
38. T. Ozawa, Polymer **12**, 1508 (1971)

Authors and Affiliations

Wenqian Zhao[1] · Richie Yang[2] · Shengfu Yang[3] · Kan Zhang[1] (ORCID)

✉ Shengfu Yang
  sfy1@le.ac.uk

✉ Kan Zhang
  zhangkan@ujs.edu.cn

[1] School of Materials Science and Engineering, Jiangsu University, Zhenjiang 200237, China

[2] King Edward VI Camp Hill School for Boys, Birmingham B14 7QJ, UK

[3] School of Chemistry, University of Leicester, Leicester LE1 7RH, UK